Effect of Degree of Substitution and Molecular Weight of Carboxymethyl Chitosan Nanoparticles on Doxorubicin Delivery

Xiaowen Shi, Yumin Du, Jianhong Yang, Baozhong Zhang, Liping Sun

Department of Environmental Science, College of Resource and Environmental Science, Wuhan University, Wuhan 430072, People's Republic of China

Received 31 May 2005; accepted 27 August 2005
DOI 10.1002/app.23040
Published online in Wiley InterScience (www.interscience.wiley.com).

ABSTRACT: The aim of this study was to evaluate the potential of carboxymethyl chitosan (CM-chitosan) nanoparticles as carriers for the anticancer drug, doxorubicin (DOX). Different kinds of CM-chitosan with various molecular weight (MW) and degree of substitution (DS) were employed to prepare nanoparticles through ionical gelification with calcium ions. Factors affecting nanoparticles formation in relation to MW and DS of CM-chitosan were discussed. By the way of dynamic light scattering (DLS), TEM, and atomic force microscopy (AFM), nanoparticles were shown to be around 200–300 nm and in a narrow distribution. FTIR revealed strong electrostatic interactions between carboxyl groups of CM-chitosan and calcium ions. DOX delivery was affected by the molecular structure of CM-chitosan. Increasing MWs of CM-chitosan from 4.50 to 38.9 kDa, DOX entrapment efficiency was enhanced from 10 to 40% and higher DS slightly improved the load of DOX. In vitro release studies showed an initial burst followed by an extended slow release. The DOX release rate was hindered by CM-chitosan with high MW and DS. These preliminary studies showed the feasibility of CM-chitosan nanoparticles to entrap DOX and the potential to deliver it as controlled release nanoparticles. © 2006 Wiley Periodicals, Inc. J Appl Polym Sci 100: 4689–4696, 2006

Key words: carboxymethyl chitosan; doxorubicin; nanoparticles; drug delivery systems

INTRODUCTION

In recent years, significant effort has been devoted to develop biodegradable nanoparticles for drug delivery, since they can be used to provide targeted delivery of drugs, to improve oral bioavailability, to sustain drug in target tissue, and to improve the stability of therapeutic agents against enzymatic degradation.[1,2] Some investigations have shown that nanoparticles are very effective in drug delivery for cancer treatment and diagnosis,[3] while reducing systemic side-effects. Nanosized carriers as vehicles for anticancer drugs have a passive targeting capability due to their enhanced permeability and retention (EPR) effect, resulting from leaky vasculature in tumor tissues and lack of lymphatic drainage.[4] Synthetic biodegradable polymers, such as poly(glycolic acid) (PGA), polylactide (PLA),[5] and their copolymers,[6,7] have been paid much attention to prepare nanopaticles because of their good biocompatibility, biodegradability, and novel drug release behavior. However, these nanoparticles are not ideal carriers for some hydrophilic anticancer drugs because of their strong hydrophobic property. Moreover, these hydrophobic particles are cleared up rapidly by mononuclear phagocytes system (MPS) after intravenous administration. To improve their hydrophilic property, the surface of nanoparticles was modified by poly(ethylene glycol) (PEG) or poly(ethylene oxide) (PEO).[8,9] Usually, these preparation procedures are complex and have the limitation to use some organic solvents or surfactants. Nanoparticles prepared from some polysaccharides under mild conditions have been a new way to obtain hydrophilic nanoparticles.

Chitosan is a biodegradable natural polymer with great potential for pharmaceutical applications because of its biocompatibility, high charge density, nontoxicity, and mucoadhesion.[10] Chitosan is insoluble in water and usually dissolves in pH acid for drug carrying. However, it is unfavorable when loading some vulnerable macromolecules. *N*,*O*-carboxymethyl chitosan (CM-chitosan) is a water soluble chitosan derivative having carboxymethyl substituents on some or both the amino and primary hydroxyl sites of the glucosamine units of the chitosan structure.[11] It was reported that CM-chitosan is nontoxic in vitro and in vivo by testing with intraperitoneal, oral, or subcutaneous treatments.[12] Because of their excellent water solubility and biocompability together with biodegradability, the ideal of making water-soluble CM-

Correspondence to: Y. Du (duyumin@whu.edu.cn).

chitosan nanoparticles becomes appealing. However, to the best of our knowledge, there is no report about nanoparticle delivery system made from CM-chitosan.

In this study, CM-chitosan nanoparticles were first prepared by gelification with calcium ions. The factors affecting nanoparticle formation were discussed and physicochemical properties have been characterized. Doxorubicin (DOX), a widely used anticancer drug in chemotherapy treatment, was chosen as a model drug. We intend to explicate the encapsulation and release of DOX from nanoparticles of CM-Chitosan related to its molecular references, i.e., molecular weight (MW) and degree of substitution (DS), which will give an insight into the alternative forms of administering DOX for the treatment of cancer.

MATERIALS AND METHODS

Materials

Chitosan (Zhejiang Aoxing Biological Product Inc., China) was refined by dissolving it in dilute acetic acid solution (1%; v/v), filtered, and precipitated with aqueous NaOH (5%; w/v), then washed to neutral and finally dried in vacuum at room temperature. The degree of deacetylation (DD) was 92% and the MW was 210 kDa. Doxorubicin hydrochloride was purchased from Mingzhi Medicine Co. (Shantou, China) and used without further purification. Aqueous solutions were prepared with double distilled water and all other chemicals were of analytical grade.

Preparation of CM-chitosan with various MW and DS

CM-chitosan with different DS were prepared based on our previous work.[13] In brief, 10 g chitosan (10 g) were frozen at −20°C in 10 mL alkali solution (40, 50, and 60%; w/w) for 12 h, then transferred to 100 mL 2-propanol, and 12.0 g $ClCH_2COOH$ was added in parts. The mixture was kept stirring at 20°C for 2 h then for another 4 h at 60°C. After dialyzing and vacuum drying, CM-chitosan was obtained. DS values of prepared products were estimated from potentiometric titrations, as 0.63, 0.82, and 0.74, respectively.[14] CM-chitosan with DS more than 1.0 was prepared by carboxymethylation twice in NaOH (50%; w/w) and the DS was determined as 1.20.

Above-prepared CM-chitosan (DS = 0.82) was degraded with hydrogen peroxide to prepared CM-chitosan with different MWs. Four milliliters of H_2O_2 (30%; v/v) was added to 100 mL CM-chitosan solution (5%; w/v) at 40°C. After predetermined time (0, 0.5, 1, and 4 h), samples were withdrawn and Na_2SO_3 was dropped in to stop the oxidation. This solution was concentrated under reduced pressure and precipitated by ethanol. Molecular weights of the prepared CM-chitosan were measured by gel-permeation chromatography (GPC), as 38.9, 13.9, 7.60, and 4.50 kDa, respectively.

Preparation of drug-free and drug-loaded CM-chitosan nanoparticles

CM-chitosan nanoparticles were obtained by ionical gelification of a CM-chitosan solution with calcium chloride. CM-chitosan with various MW and DS was dissolved in double distilled water at predetermined concentration. Then 2 mL of $CaCl_2$ solution was added to 5 mL of CM-chitosan solution under mild magnetic stirring, and the system changed spontaneously from a clear solution to an opalescent emulsion (Tyndall effect), which was further measured by TEM as nanoparticles. Without specific depiction, the parameter of CM-chitosan used and the preparation formulation were as follows: MW 38.9 kDa and DS 0.82, concentration 500 μg/mL; the concentration of $CaCl_2$ was 1.0 mg/mL. The DOX loading nanoparticles were formed in the same way by adding $CaCl_2$ solution to CM-chitosan solution containing 20 μg/mL DOX. The nanoparticles were separated by centrifugation with 20,000 × g (3k30, Sigma, USA) at 4°C for 30 min and lyophilized for further characterization and release study.

Morphology and structure characterization of the nanoparticles

FTIR spectra were recorded with KBr pellets on a 170 SX Fourier transform-infrared spectrometer (USA), sixteen scans at a resolution of 4 cm^{-1} were averaged and referenced against air.

TEM (100 CX II, Japan) was used to observe the morphology of the CM-chitosan nanoparticles. Samples were placed onto copper grill and dried at room temperature, then examined without being stained.

The mean size and size distribution of the CM-chitosan nanoparticles were measured by dynamic light scattering (DLS) (Zetasize; 3000 HS, Malvern, UK). All measurements were done with a wavelength of 633.0 nm at 25°C with an angle detection of 90°. Each sample was repeatedly measured three times.

Atomic force microscopy (AFM, MI Picoscan) was used for close visualization of the CM-chitosan nanoparticles deposited on mica substrates and was operated in the contact mode.

X-ray diffraction was recorded by a Shimadzu Lab-XRD-6000 diffractometer and used a CuK_α as target at 40 kV and 30 mA.

Fluorimetric analysis

Reagent concentrations were fixed for each assay. DOX concentration was fixed as 20 μg/mL and CM-chitosan and calcium ions were maintained constant at 0.36 and 0.29 mg/mL, respectively. DOX emission

spectra were recorded from 500 to 700 nm at a fixed excitation of 480 nm with excitation and emission slit widths of 5 nm. Spectra were recorded at a scan speed of 200 nm/min.

Evaluation of DOX encapsulation

In the determination of the encapsulation efficiency (EE), the DOX-loaded CM-chitosan nanoparticles were separated from the aqueous suspension medium by ultracentrifugation with 20,000 × *g* at 4°C for 30 min. The amount of free DOX in the clear supertant was determined using Shimadzu HPLC system (Japan) equipped with a reverse-phase column C18 (250 × 4.6 mm^2). The elution was a mixture solution containing 25 m*M* $NH_4H_2PO_4$–30 m*M* H_3PO_4 phosphate buffer, methanol, and acetonitrile (3:5:2; v/v). The flow rate was maintained at 1 mL/min and the eluent was monitored with UV detector at 233 nm. All measurements were performed in triplicate.

EE of DOX loaded and loading capacity (LC) were calculated from the following equation[15]:

$$EE = (A - B)/A \times 100$$

$$LC = (A - B)/C \times 100$$

where, *A* is the total amount of DOX added; *B* is the free amount of DOX in suspension; and *C* is the nanoparticles weight in dry state.

Evaluation of in vitro DOX release

Ten milligrams of DOX-loaded CM-chitosan nanoparticles were resuspended in 10 mL 0.01*M* phosphate buffered saline (PBS, pH = 7.4) and kept at 37°C with continuous shaking at 100 rpm. After a predetermined period, 1 mL of the sample medium was periodically removed and replaced by the same quantity of release medium to maintain the original volume, the amount of released DOX was analyzed by HPLC measurement based on the former described method. The DOX release experiments were performed in triplicate, and nonloaded nanoparticles was used as calibration.

RESULTS AND DISCUSSION

Factors affecting nanoparticle formation

To determine the nanoparticles formation zone, preliminary experiments adopted the protocol developed in alginate nanoparticles by ionic gelation with calcium ions were carried out.[16] The initial concentration of CM-chitosan was 0.5–2 mg/mL and calcium concentration was between 0.5 and 8.0 mg/mL. It can be observed that the formation of nanoparticles was only limited in a narrow concentration range of CM-chitosan and calcium ions [Fig. 1(a)]. When the concentration of CM-chitosan increased, more calcium ions were needed to form opalescent suspension. Minimum size of the particles was obtained at the lowest CM-chitosan concentration, and the mean size, and size distribution increased with the increase of either the CM-chitosan or the $CaCl_2$ concentration. Similar trend was also found in other study on chitosan nanoparticles gelated by TPP.[17]

MW and DS also play an important role in the nanoparticle formation. With the increased MW of CM-chitosan, less calcium ions were needed for nanoparticle formation [Fig. 1(b)]. This can be explained that longer molecular chain was much easier to roll-up when coordinated with calcium ions, compared to shorter chains. Figure 1(c) shows that as the DS of CM-chitosan increased, the concentration of calcium ions for nanoparticle formation decreased. High DS value means large negative charge density on CM-chitosan chain, and so calcium ions can easily coordinate with CM-chitosan by electrostatic attractive forces, thus leading to the formation of nanoparticles. The optimum preparation conditions related to specific MW or DS were listed in Table I.

Morphology and size distribution of nanoparticles

Because particle size has a crucial impact on the *in vivo* fate of the particulate drug delivery system,[18] the particle size control is of great importance for drug carriers. Size distribution of typical CM-chitosan nanoparticles by DLS demonstrated a narrow distribution and the polydispersity index (PI) lower than 0.1 was identified. The small PI value indicated a homogeneous dispersion of CM-chitosan nanoparticles.

Figure 2 shows the typical TEM image of prepared CM-chitosan nanoparticles, which can be seen as spherical in shape and no conglomeration was found. The AFM technique was adopted to study the detailed surface morphology of nanoparticles. It confirmed that there was no aggregation or adhesion among the nanoparticles [Fig. 3(a)]. Zoom-in image of a spherical nanoparticle revealed the fine surface structure [Fig. 3(b)]; it can be seen that the nanoparticle had a very distinct boundary, a dense, and rather smooth surface that was found from AFM image, which could be seen closely.

It should be noted that MW and DS of CM-chitosan had obvious influence on the particle size. As shown in Table I, the increase of MW led to larger particle size, this can be easily explained by longer molecular chain entangled together giving rise to bigger nanoparticles. Similar trends were observed for chitosan systems.[19,20] Interestingly, the increase of DS decrease the diameter slightly, which may be caused by more compact structure formed between high DS CM-chitosan and calcium ions.

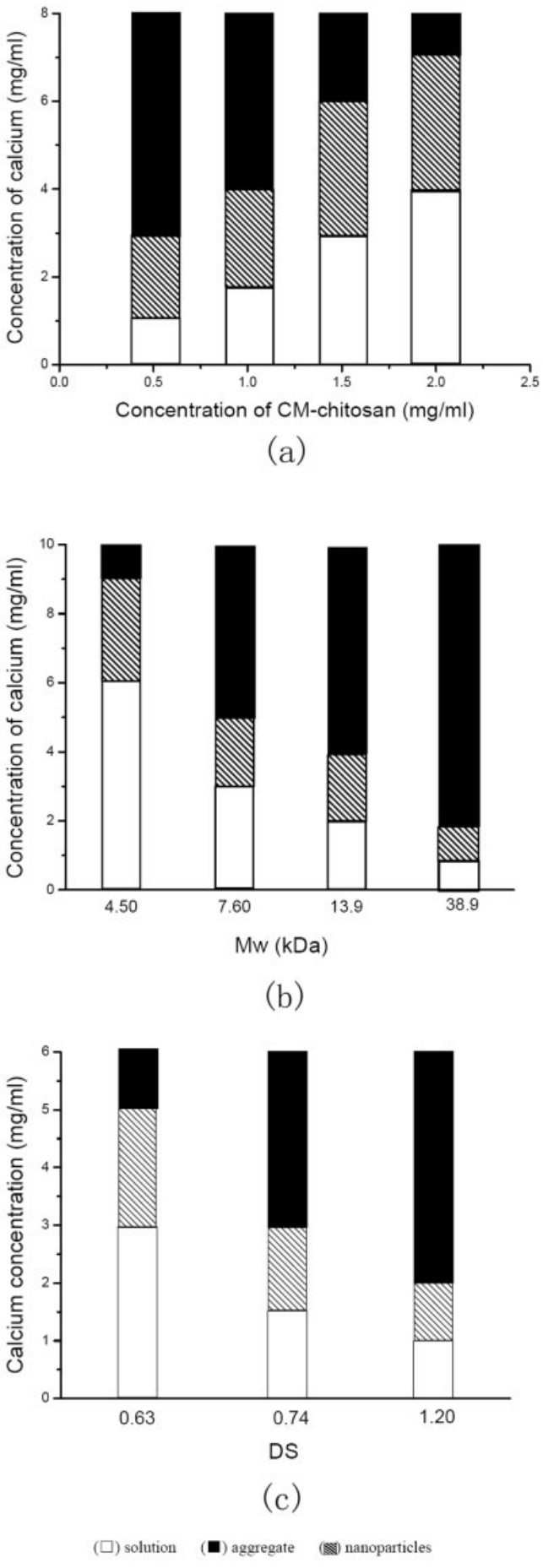

We also found CM-chitosan nanoparticles were considerably stable. Formed complex suspension was kept in room temperature for 1 week, and there were no significant changes in the nanoparticle size throughout the period and no particle agglomeration was observed. The high stability may be caused by electrostatic repulsions between nanoparticles.

FTIR spectra and XRD analysis

To study the interactions between CM-chitosan and calcium ions, nanoparticles were characterized by FTIR. Figure 4 shows the spectras of CM-chitosan and its nanoparticles. In general, the absorption band of protonized carboxylic group occurs around 1740 cm^{-1}, whereas the ionized stretching band occurs near 1600 cm^{-1}. In nanoparticle formation, no absorption band was found in the region of 1740 cm^{-1} and the presence of strong bands were observed at 1600 and 1418 cm^{-1}, which belonged to the asymmetric and symmetric stretching of carboxylate anion, respectively.[21] It indicated that the carboxyl group in CM-chitosan had a high degree of anionic characteristic. Compared with the spectra of CM-chitosan, the asymmetric stretching vibration of COO^- groups in the spectrum of nanoparticles shifted to higher wavenumber, while the symmetric stretching vibration shifted to lower wavenumber, indicating that strong interactions existed between ionized carboxyl groups and calcium ions. The broad band at 3420 cm^{-1} corresponded to the amine and hydroxyl groups. There was little change in the shape and wavenumber in CM-chitosan and nanoparticles, which suggested that neither the -OH nor the $-NH_2$ group are involved in the coordination of calcium ions and CM-chitosan.[22]

The X-ray diffraction patterns of CM-chitosan and calcium ions gelification nanoparticles are shown in Figure 5. CM-chitosan exhibited a crystalline peak at $2\theta = 19°$, while this crystalline peak completely disappeared in the pattern of the nanoparticles. The hydrogen bonding in CM-chitosan may be broken up through coordinating with calcium ions and then results in the amorphous structure of the nanoparticles.

DOX loading within nanoparticles

The encapsulation of DOX in nanoparticles would absolutely cause change to the fluorescence profiles of DOX. Fluorescences of DOX emission spectra before and after nanoparticle formation are shown in Figure 6. In control studies, no detectable emission was noted

Figure 1 Nanoparticle formation zone for various CM-chitosan and calcium ions concentration (a), CM-chitosan with different MW (b), and DS (c). 72 × 199 mm^2 (300 × 300 DPI).

TABLE I
Typical Mean Particle Sizes and Polydispersity Index (PI) of CM-Chitosan Nanoparticles Determined by DLS (n = 3)

CM-chitosan		CM-chitosan	$CaCl_2$	Particle size	
MW (kDa)	DS	(mg/mL)	(mg/mL)	(nm)	PI
38.9			1.0	272 ± 35	0.089
13.9	ca. 0.8		2.0	270 ± 23	0.101
7.60			3.0	253 ± 17	0.042
4.50		0.5	6.0	207 ± 25	0.022
	0.63		3.0	268 ± 19	0.072
ca. 39.0	0.74		1.5	252 ± 33	0.086
25.5	1.20		1.0	243 ± 21	0.069

for individual CM-chitosan and calcium ions solutions over the chosen wavelength range at the concentrations tested. As can be seen, the DOX peak at 565 nm was reduced to 23% upon incubating with CM-chitosan. The protonable groups in the DOX molecule were expected to interact with the carboxyl groups of CM-chitosan, which benefited the loading of DOX in the nanopaticles. Subsequent addition of calcium ions increased the intensity of the 565 nm peak to 69% of the original DOX absorbance. The complex between DOX and CM-chitosan appeared to be partially dissociated by the addition of calcium ions, which implied that high DOX encapsulation efficiency could only be obtained in the case of low calcium concentration. Furthermore, no spectral changes in the DOX peak were observed for the samples, the preservation of the fluorescence signature suggested that DOX structure was retained following encapsulation in CM-chitosan nanoparticles. DOX encapsulation was also visibly apparent with these nanoparticles, which formed a dense red pellet upon centrifugation.

The effects of MWs of CM-chitosan on DOX encapsulation efficiency can be seen in Figure 7. The EE of DOX increased from 10 to 40% with increased MW of CM-chitosan. As stated above, less calcium ions were needed for high MW CM-chitosan. CM-chitosan with various MWs and similar DS have the same functional groups.[23] For the high MW CM-chitosan, there are more carboxyl groups left for DOX, and so the encapsulation efficiency is much higher. On the other hand, compared with short molecular chains of low molecule weight CM-chitosan, the relatively longer chain makes the encapsulation of DOX much easier due to some physical interaction such as adsorption and entrapment.

A comparison of the DOX encapsulation efficiencies for different DS CM-chitosan nanoparticle is shown in Figure 8. Increased DS of CM-chitosan led to higher encapsulation efficiency. As revealed in our previous nanoparticle preparation study, less calcium ions were added with high DS CM-chitosan to form nanoparticles. Therefore, CM-chitosan with higher DS had more functional groups that can interact with DOX. Despite surplus carboxyl groups on chains, mean encapsulation efficiencies increased only slightly with increase of DS with all encapsulation efficiencies be-

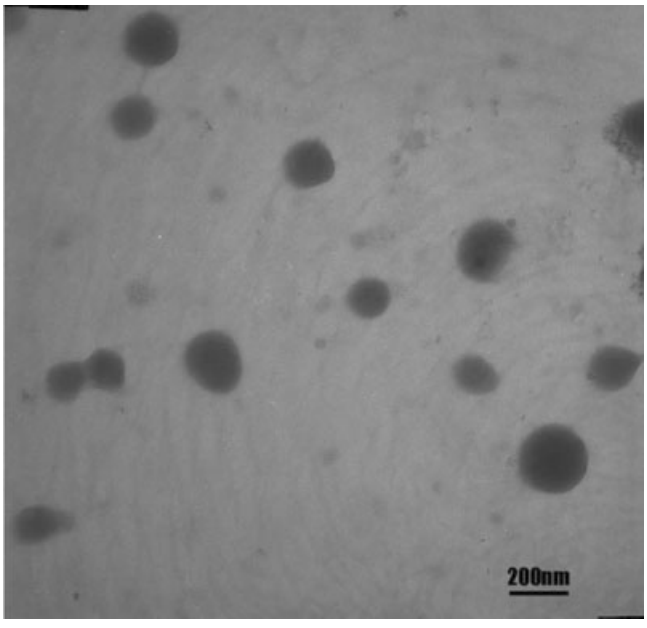

Figure 2 TEM of CM-chitosan nanoparticles (MW = 38.9 kDa; CM-chitosan, 0.5 mg/mL; calcium ions, 1.0 mg/mL). 65 × 55 mm^2 (300 × 300 DPI).

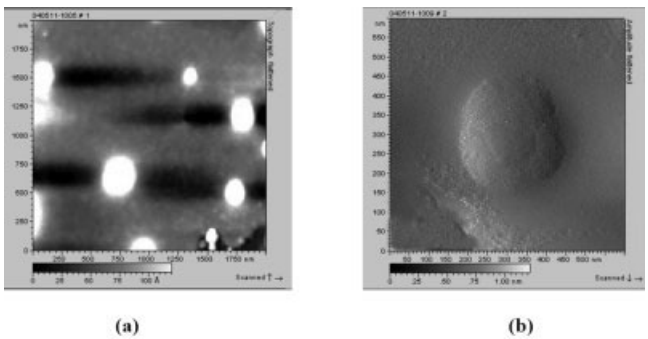

Figure 3 AFM image of CM-chitosan nanoparticles (a) and its zoom-in picture (b). 89 × 48 mm^2 (300 × 300 DPI).

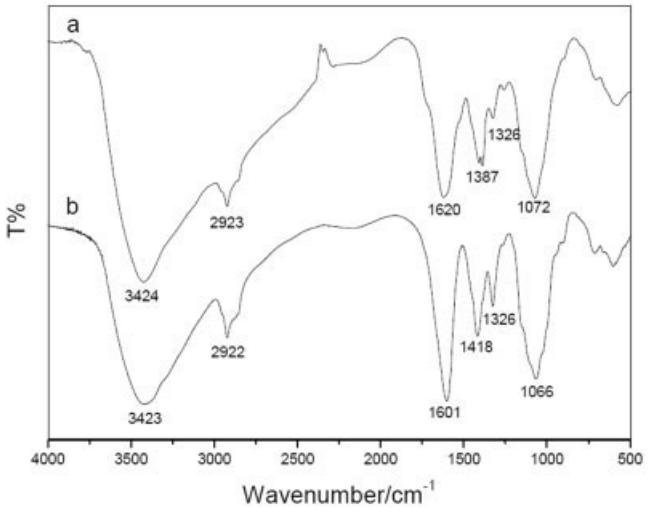

Figure 4 FTIR of CM-chitosan nanoparticles (a) and CM-chitosan (b). 67 × 54 mm^2 (300 × 300 DPI).

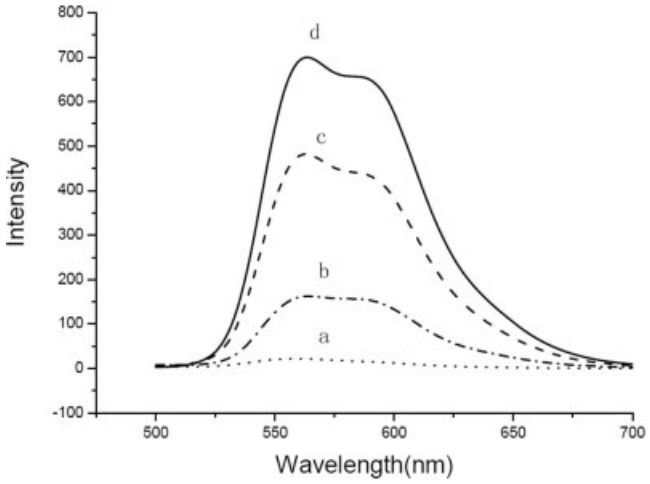

Figure 6 Fluorescence emission spectra of: CM-chitosan + calcium ions solution (a); DOX + CM-chitosan solution (b); DOX encapsulated in CM-chitosan nanoparticles (c); and DOX solution in water (d). 66 × 51 mm^2 (300 × 300 DPI).

tween 26 and 36%. This indicates that the load of DOX in nanoparticles was mainly affected by MW rather than the DS of CM-chitosan. The DOX loading results by various MW and DS suggested that high DOX load happens with CM-chitosan with high MW and DS value. The load capability (4.2%, w/w) of the CM-chitosan nanoparticles for DOX is relatively high and comparable to that obtained for other hydrogel particle systems.[24,25]

In vitro DOX release

The in vitro release profile of DOX loaded CM-chitosan nanoparticles with various MWs in 0.01*M* PBS (pH 7.4) is shown in Figure 9. The particles with MW 4.50 kDa showed a burst release of 70% at first 2 h, followed by an additional release of 4.0% over the next 2 days. For nanoparticles prepared from higher MW, reduced initial burst release was observed and negligible DOX increases in release detected over the proceeding 3 days. The initial phase of release is logically attributed to the DOX located at the surface of the particles, while the remainder of the unreleased DOX was assumed to be well entrapped within nanoparticles and tightly associated to the CM-chitosan molecules, probably as an ionic complex with carboxyl group. It is obvious that the release of lower MW is much faster, and this was as expected because nanoparticles with low MW has smaller size and larger volume-to-surface area, which speeded DOX initial release from surface. Since the interaction between

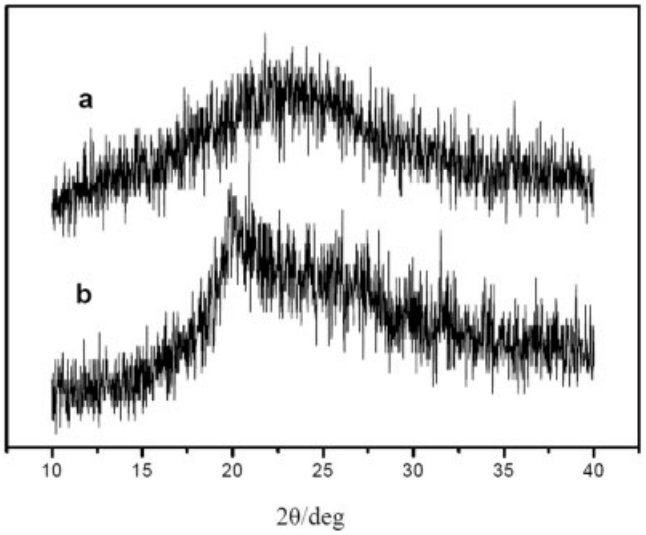

Figure 5 XRD patterns of CM-chitosan nanoparticles (a) and CM-chitosan (b). 65 × 53 mm^2 (300 × 300 DPI).

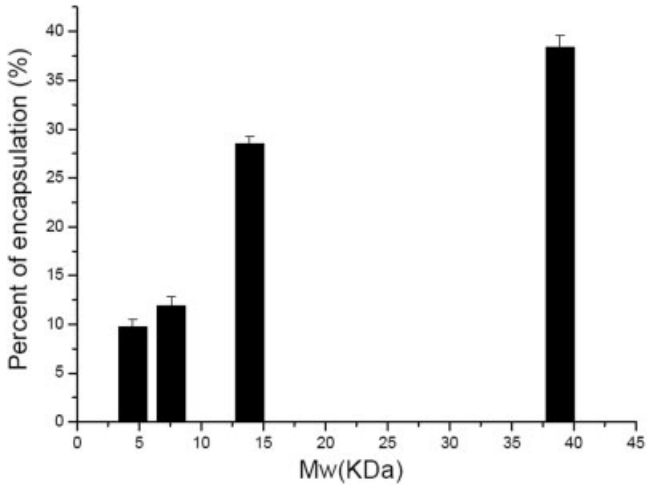

Figure 7 DOX encapsulation efficiency of CM-chitosan with various MW (n = 3) 64 × 50 mm^2 (300 × 300 DPI).

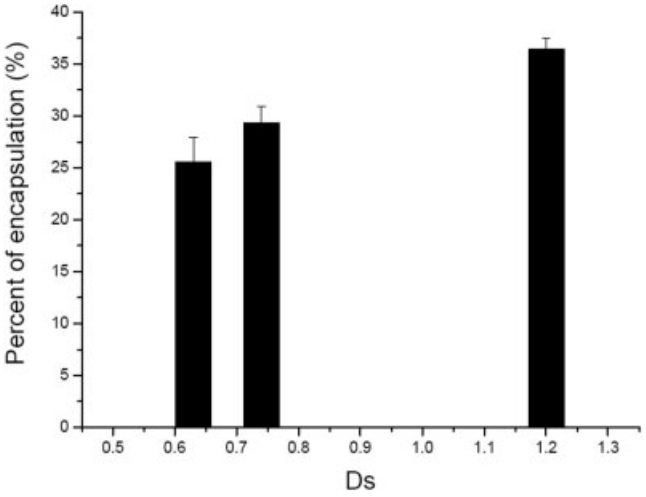

Figure 8 DOX encapsulation efficiency of CM-chitosan with various DS (n = 3). 64 × 50 mm^2 (300 × 300 DPI).

DOX and CM-chitosan seems to be quite stable, any extended drug release would be a result of degradation of CM-chitosan or by release of DOX complexed on the particle surface. It has been shown high MW polymer have slow degradation rate, thus preventing the drug from diffusing from the physicopolymer matrix into the aqueous solution due to increased chain packing and rigidity.[26]

Nanoparticles prepared from CM-chitosan with various DS displayed similar DOX release pattern (Fig. 10). For all the samples, an initial burst of 36–50% was observed within the first 2 h of incubation. However, after the initial burst release, drug release from

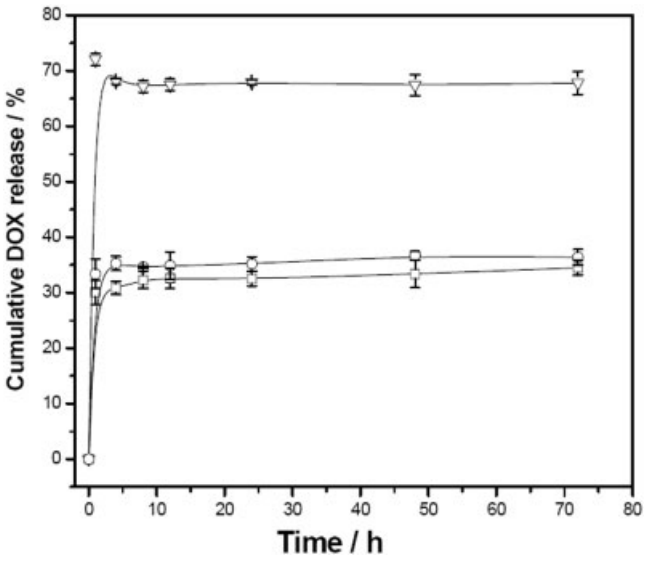

Figure 9 The influence of MW of CM-chitosan on DOX release behavior: (▽) MW = 4.50 kDa, LC = 0.96%; (○) MW = 7.60 kDa, LC = 2.8%; (□) MW = 13.9 kDa, LC = 3.4%. 58 × 51 mm^2 (300 × 300 DPI).

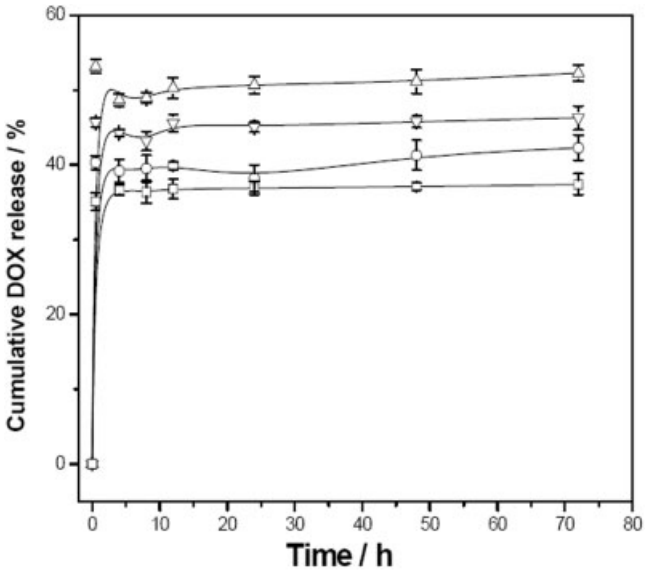

Figure 10 The influence of DS of CM-chitosan on DOX release behavior: (△) DS = 0.63, LC = 2.9%; (▽) DS = 0.74, LC = 3.4%; (□) DS = 0.82, LC = 4.2%; (○) DS = 1.20, LC = 3.8%. 52 × 46 mm^2 (300 × 300 DPI).

the particles became rather low and DOX release ranged from 40 to 53% in 3 days. As the DS of CM-chitosan increased, the release rate decreased. This observation may be related to the Coulombic interactions including hydrogen bonding and hydrophobic interactions that bound the drug to the CM-chitosan. Higher DS of CM-chitosan are expected to provide more compact nanoparticles because of larger number of carboxyl groups of CM-chitosan gelated with calcium ions. However, when DS increased to 1.20, the release rate increased instead compared with the nanoparticles with DS 0.82. This phenomenon probably related to MW difference between these two samples, the MW of CM-chitosan(DS 1.20) was lower than that of CM-chitosan(DS 0.82). In this case, MW may play an important role and cause the observed difference. Therefore, the release rate pattern of DOX from biodegradable nanoparticles of CM-chitosan can thus be tailored by choosing the molecular structure parameters such as MW and substitution.

CONCLUSIONS

In the present study, CM-chitosan nanoparticles as colloidal carriers for the delivery of DOX, a commonly used anticancer cationic drug were investigated. The physicochemical structure of the nanoparticles gelation with calcium ions was characterized. The nanoparticle preparation was affected by environmental parameters as well as molecular parameters of CM-chitosan. The DS and MW of CM-chitosan play an important role in DOX delivery. CM-chitosan with higher MW and DS enhanced DOX loading to 4.2%

and showed smaller release over the test period in vitro. Further experimentational testing of the circulate time and location in vivo is necessary to clarify the potential of CM-chitosan nanoparticles as controlled release nanoparticles.

References

1. Lisa, B. P. Int J Pharm 1995, 116, 1.
2. Soppimath, K. S.; Aminabhavi, T. M.; Kulkarni, A. R.; Rudzinski, W. E. J Controlled Release 2001, 70, 1.
3. Brigger, I.; Dubernet, C.; Couvreur, P. Adv Drug Delivery Rev 2002, 54, 631.
4. Kong, G.; Braum, R. D.; Dewhirst, M. W. Cancer Res 2001, 61, 3027.
5. Zambaux, M. F.; Bonneaux, F.; Gref, R.; Dellacherie, E.; Vigneron, C. J Controlled Release 1999, 60, 179.
6. Fonseca, C.; Simoes, S.; Gaspar, R. J Controlled Release 2002, 83, 273.
7. Liu, Y.; Guo, L. K.; Huang, L.; Deng, X. M. J Appl Polym Sci 2003, 90, 3150.
8. Storm, G.; Belliot, S. O.; Deamen, T.; Lasic, D. D. Adv Drug Delivery Rev 1995, 17, 31.
9. Vittaz, M.; Bazile, D.; Spenlehauer, G.; Verrecchia, T.; Veillard, M.; Puisieux, F.; Labbarre, D. Biomaterials 1996, 17, 1575.
10. Sinha, V. R.; Singla, A. K.; Wadhawan, S.; Kaushik, R.; Kumria, R.; Bansal, K.; Dhawan, S. Int J Pharm 2004, 274, 1.
11. Hayes, E. R. U.S. Pat. 4,619,995 (1986).
12. Kennedy, R.; Costain, D. J.; McAlister, V. C.; Lee, T. D. G. Surgery 1996, 120, 866.
13. Chen, L. Y.; Tian, Z. G.; Du, Y. M. Biomaterials 2004, 25, 3725.
14. Muzzarelli, R.; Tanfani, F.; Emanuelli, M.; Mariotti, S. Carbohydr Res 1982, 107, 199.
15. Xu, Y. M.; Du, Y. M. Int J Pharm 2003, 250, 215.
16. Rajaonarivony, M.; Vauthier, C.; Courraze, G.; Puisieux, F.; Couvreur, P. J Pharm Sci 1993, 82, 912.
17. Calvo, P.; Remunan-lopez, C. R.; Vila-jato, J. L.; Alonso, M. J. J Appl Polym Sci 1997, 63, 125.
18. Moghimi, S. M.; Hunter, A. C.; Murray, J. C. Pharmacol Rev 2001, 53, 283.
19. Huang, M.; Khor, E.; Lim, L. Y. Pharm Res 2004, 21, 344.
20. Janes, K. A.; Fresneau, M. P.; Marazuela, A.; Fabra, A.; Alonso, M. J. J Controlled Release 2001, 73, 255.
21. Muzzarelli, R. A. A.; Tanfani, F.; Emanuelli, M.; Mariotti, S. Carbohydr Res 1982, 107, 199.
22. Tang, L. G.; Hon, D. N.-S. J Appl Polym Sci 2001, 79, 1476.
23. Flory, P. J. Principles of Polymer Chemistry; Cornell University Press: New York, 1953.
24. Janes, K. A.; Alonso, M. J. J Appl Polym Sci 2003, 88, 2769.
25. Leo, E.; Vandelli, M. A.; Cameroni, R.; Forni, F. Int J Pharm 1997, 155, 75.
26. Zhang, H.; Neau, S. H. Biomaterials 2002, 23, 2761.